A New Method to Assess the Volume of Volcanic Landforms and Associated Deposits

Mathieu Perton[1], Guillermo Cisneros Máximo[2], Silvestre Cardona-Melchor[2], Xavier Bolós[2], Martha Gabriela Gómez-Vasconcelos[3], Susana Osorio-Ocampo[2], Denis Ramón Avellán Lopéz[4], José Luis Macías[2]

[1]Instituto de Ingeniería, Universidad Nacional Autónoma de México, Circuito Escolar s/n, Cd Universitaria, Coyoacán 04510, CDMX, México, (Corresponding autor, email: mathieu.perton@gmail.com).

[2]Instituto de Geofísica, Universidad Nacional Autónoma de México, Antigua Carretera a Pátzcuaro 8701, 58190, Morelia, Michoacán, México.

[3]CONACYT–Instituto de Investigaciones en Ciencias de la Tierra, Universidad Michoacana de San Nicolás de Hidalgo, Santiago Tapia 403, 58000, Morelia, Michoacán, México.

[4]CONACYT-Instituto de Geofísica, Universidad Nacional Autónoma de México, Antigua Carretera a Pátzcuaro 8701, 58190, Morelia, Michoacán, México.

Corresponding author: Mathieu Perton (mathieu.perton@gmail.com)

Key Points:

- Volume computation
- Volcanoes volume
- Lava volume

Abstract

The calculation of volcanic deposit volume has been drastically improved from two decades because of the apparition of detailed digital elevation models. We proposed here an executable program with its graphical user interface to compute them easily. Contrary to recent calculations that assess the base of the volcano by using a contour interpolation through Delaunay triangulation and which obtain generally flat basement, we also consider the surrounding slopes to obtain the hidden volume in paleo-depression and then better assess basement topography. We also propose solutions to correct some basement elevations that are assessed above the actual topography when using recent methods. We validated the method with the Paricutin case. We also demonstrate the ability to retrieve hidden volumes covered by younger volcanoes in the case of the volcanic complex La Nieve.

1. Introduction

The volume of a volcanic deposit is an important quantitative parameter to constrain the magnitude of the eruption, its volcanic explosive index (Newhall & Self, 1982) and its hazard (Martí, 2017). However, volcanic eruptions follow complex series of explosive and effusive processes, involve aggradational processes such as deposition of pyroclasts and lavas, and degradational processes by erosion and transport such as lahars, landslides or debris avalanches (Jean Claude Thouret et al., 2014). Then, the volume must better be seen as a dynamic parameter that is important to finely estimate over time in order to characterize, jointly with other volcanic morphometric parameters, the tectonic/structural settings, flux dynamics, volcano magma compositions and eruptive styles, and erosion rates (Bagnardi et al., 2016; Cotton, 1944; Davidson & De Silva, 2000; Francis, 1993; Grosse et al., 2012; Kereszturi et al., 2013; Rodriguez-Gonzalez et al., 2010; J.C. Thouret, 1999).

Historically, lava volumes were calculated from the area and the estimated mean thickness of the lava flow (Hulme, 1974; Romano & Sturiale, 1982; Wadge et al., 1975; Wilson & Head, 1983). The estimation of cinder cone volumes used the geometric formulae of the truncated cone (Stevens et al., 1999a; Wood, 1980). Because these methods are only based on observation, they have serious limitations. During the last decade, the extended use of Geographic Information Systems (GIS) has improved the morphometrical modeling of volcanic structures and several methods for volume estimation consider the post-eruption digital elevation models (DEM) and when available the pre-eruption DEM (Albino et al., 2015; Kubanek et al., 2015; Stevens et al., 1999b). If these latter are not known, geological information is added to retrieve the paleo-topography (Bagnardi et al., 2016; Dibacto et al., 2020; Germa et al., 2015; Hildreth et al., 2003; Lahitte et al., 2012; Rodriguez-Gonzalez et al., 2010, 2012; Székely & Karátson, 2004). It arises also that the post-eruption DEM is not fully available, as when volcanoes are degraded or when several volcanoes are superimposed which is typical of monogenetic volcanic fields (scoria cones, domes, lava flows, etc.). In the most recent volume estimation methods, the paleo topographies are mainly retrieved by interpolating the actual volcano contour. This generally leads to paleo topographies that may erroneously stand above the actual topography. Here, we show that some of these artefacts are due to a bad evaluation of the contour and we propose an efficient and automatic method to additionally constrain the paleo topographies by considering the slope around the volcano or lavas and the actual topography.

We first present the details of the method and validate it with the Paricutin Volcano case by comparing the real paleo topography with the one assessed. Then we apply the method to an imbricated volcanic complex and reveal several paleo-topographies.

2. The Methods

In its essence, the method is quite simple and consists of integrating the volume between the elevation of the base (the paleo topography defined by z_{base}) of the volcano or the lava and the elevation of its actual topography (z_{top}). For the topography, we use any available DEM of the area that is delimited by a contour line (C). The contour can be a single closed contour or can be multiple by enclosing several internal empty areas, e.g. when the lava has had to bypass small obstacles. The DEM is generally given in function of a regular square grid in local UTM coordinates and the area of each cell is denoted as ΔA. In latitude and longitude, the axes are equally distributed in degree which means that the grid is irregular. In that case, ΔA is taken implicitly as a function of the position. Finally, the volume is computed as the sum of all the subvolumes of the columns at each position of the grid:

$$V = \sum (z_{top} - z_{base}) \Delta A. \quad (1)$$

The difficulties are in fact two: determining the cells that belong to the volcano or the lava and assessing correctly the elevation of the basis.

In order to illustrate the method and to evaluate the error when assessing the volume, we choose the scoria cone of Paricutin volcano (Michoacán, Mexico). It is in the southwest part of the Michoacán-Guanajuato Volcanic Field, 25 km apart from Uruapan city and is the youngest volcano of this field. The volcano was formed during an eruption that lasted 9 years from February 20 1943 to March 4 1952 (Luhr & Simkin, 1993). It covers an area of 233 km^2 including lavas, scoria cones and fallout tephra from the isopach map obtained after the eruption (Segerstrom, 1950). These lava flows buried the towns of Parícutin-Combutzio and San Juan Parangaricutiro. The contemporaneous formation and evolution of this volcano represents a perfect case study for understanding the origin, eruption dynamics, and evolution of monogenetic scoria cones (Larrea et al., 2017). Here, we take advantage of the known pre-eruption topography to evaluate the exact volume and to evaluate the error when assessing the volume without considering this information.

The topography before the eruption, denoted T_1 and shown in *Figure1*a, was deduced from the digitization of the map of 5 m elevation isopleths done in 1934 by Cia Mexicana Aerofoto and processed by Kenneth Segerstrom of the Geological Survey. The topography after the eruption, denoted T_2 and shown in *Figure1*b, was deduced similarly from a map established in 1952 but from INEGI. Both DEM have a horizontal resolution of 20 m by 20 m. The elevation difference between the two topographies is shown in *Figure1*c. The positive (resp. negative) elevation differences appear as colors between green and maroon (resp. red color). The areas at the southwest corner where the colors oscillate rapidly between red and green (southwest and northeast corners) correspond to small elevation differences. They are interpreted as numerical errors since they are in average centered around zero with a standard deviation of $\delta\varepsilon$= 0.25 m, and with a maximum elevation error of $\varepsilon_{max} = 1.6$ m. They are relatively low regarding the vertical sampling of the initial maps (5 m contour interval) and might be due to the digitization, interpolation and georeferencing methods. The larger areas where the colors oscillate more slowly (northwest, northeast and southeast corners) are due to the presence of a cover made by the modern soil and reworked tephra transported by rain and to depression related to new urban settling. We confirmed that these depressions and humps increase through time by using more recent DEM.

In this study, we used two different contours. The first one is determined by following the contour of the lava, as it is usually done in the case of old volcanoes. This contour is denoted as C_1 and is shown as gray lines in *Figure 1*c. The second contour denoted C_2 shown as black lines in the same figure, was determined from the positions where the elevation difference between the topography after and before the eruption is larger than the error previously estimated ($\Delta z > \delta\varepsilon$). The two contours differ strongly, and their influence on the volume calculations is discussed after.

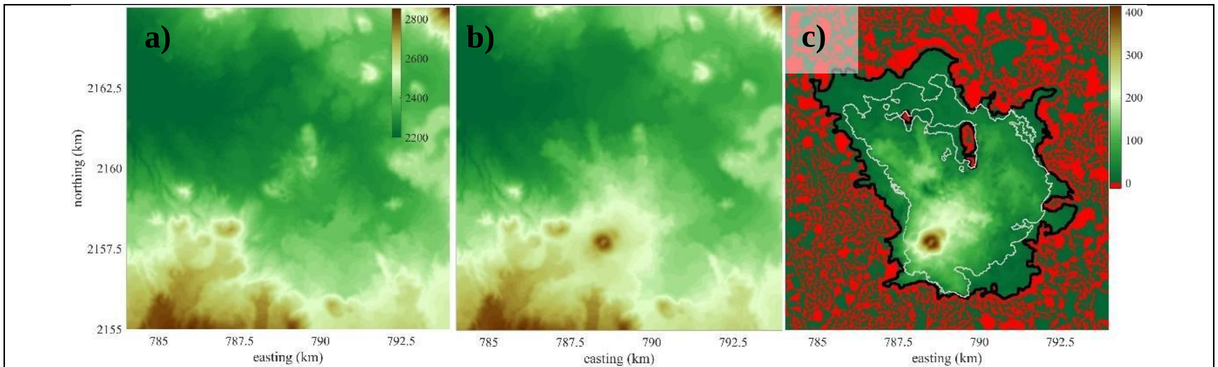

Figure1: Top view of a) the pre-eruption Parícutin topography, b) the post-eruption topography, c) the elevation difference between the post and pre-eruption topography. Color scale is the same for a) and b) but is different in c) where the red color displays the negative elevation difference. Additionally, we superimposed the contour of lava (gray lines) and the contour of significant (>1.6 m) elevation difference (black line). The maps are expressed in the 13Q UTM zone.

2.1. Determining the internal cells

To determine the internal cells, we first transform the lineal contour as a contour of cells (Figure 2a). To that purpose, we resample the line contour (shown by red points) by linear interpolation (black points) so that the distance between two contiguous points of the contour is less than the length of a cell side (here the cells are squares) and identify then the cells (grey squares) where the points stand. Consequently, there is no gap between contiguous cells in direction x or y. Somes cells crossed by the contour might however be missed. For example, the cell colored in green is crossed by a short contour segment but since no point of the contour belongs to that cell, it is not considered as part of the cell contour. Nonetheless, those cells are insignificant regarding the volume or the area. The second step consists in identifying the internal and external parts of the contour for each value of x (Figure 2b). All the cells of the contours are then indexed consecutively along the contour. Then, we identify all the cells of the contour that have the same abscissa, and the cells of contiguous indexes are grouped together. The resulting packets, represented as green circles, are numbered. The internal parts of the contour are identified between the odd and even numbers. However, if the cells before and after a packet have the same y, the packet is discarded because it consists of a tangent of the border, as illustrated in the zoom of Figure2b.

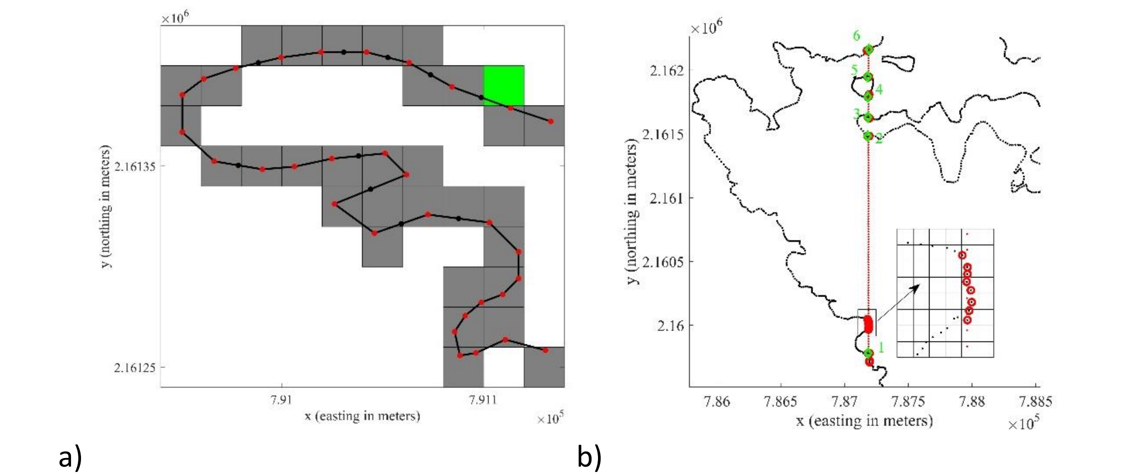

Figure2: a) The contour of points (red dots) is interpolated (black dots) and converted in a contour of cells (gray squares). Only the positions of the points are considered for the identification of the cells and not the in-between segments (e.g. the green cell). b) Identification of the internal and external parts. We first find the cells at a given *x* (red dots) and identify the cells of the contour (black points) that belong to that *x* (red circles in the zoom). We group the contiguous points of the contour (green circles) and exclude the groups that correspond to an inflexion of the contour (see zoom). Then we number the groups (green numbers) and the internal parts consists in the cells that are between odd and even groups.

2.2. Assessing the elevation of the basis

Once the internal topography is identified, we tested several strategies to compute the volume.

The first strategy (S_1), which is similar to that shown in (Favalli et al., 2009), is a simple 3D interpolation between all the points of the contour (the scattered or Delaunay triangulation of (Amidror, 2002; Matlab, 2020) generating a function of differentiability class C^1. However, some of the points of the basis result with an elevation higher than their corresponding actual topographic elevation (i.e. at the same horizontal position). Some of these problematic points can be solved by changing the interpolation method for a function of differentiability class C^0, but the basement result is generally not realistic. We identified some examples in which the problematic points were located close to the contour and that the interpolation issue was mainly due to a wrong contour identification. Choosing a slightly different contour generally solves the interpolation issue. Then, we offer the possibility for the user to visualize the problematic points and to potentially identify the wrong parts of the contour.

Alternatively, we can also suppose that the horizontal contour location is correct but that some of the contour points may have little error on their elevation, as discussed previously, and that these errors may lead to problematic points too. Then, we impose that the basement is just below the actual topography by fixing the problematic points elevation to be 2 m below their respective actual topography elevation. The 2 m value is taken sufficiently small to not introduce large changes and is considered according to a rounded value of ε_{max}. We then interpolate again the basis topography by considering these points as part of it and iterate the interpolation until all the points of the base stand below the actual topography. The advantage of this method is only to solve these problematic points and to produce a rapid evaluation of the base, but it clearly lacks justifications.

In the second strategy (S_2), we look to the topography surrounding the contour in order to extrapolate their slopes below the volcano landform topography and then to better assess the basis. To that purpose, we consider points all around the contour and outside of the area: at least 400 m in any directions x or y and at maximum 1/5 times the horizontal length in the directions x or y between the extrema positions of the contours in these directions (e.g. 1/5 of the length between points 1 and 6 in Fig2). All these points form a thick band contour. The basis is then evaluated by using the Biharmonic spline interpolation ((Matlab, 2020) griddata method) of this band contour which presents a differentiability class C^2. But, due to memory limitation, we reduce the number of points in the external contour. In our hardware configuration (Z440 workstation with 4 Gb of RAM), it was taken as 10^4 points. The reduction is made by eliminating one point over two in x and y directions. This operation is repeatedly performed until we verify the criterium. The simultaneous consideration of the positions of the contour and of its derivative allows, in fact, a better assessment of the volume of volcanoes or lava, as it will be discussed in the next paragraph, but the presence of problematic points remains as in S_1. We then used the same resolution procedure as in the first strategy.

Finally, we developed the third strategy (S_3), by using the same interpolation scheme as S_2, but by automatically modifying the contour so that problematic points disappear. Moving automatically the points of the contour might result in a complicated and hazardous approach. Therefore, we rather prefer to remove the points of the band contour that lead to the problematic points. These points correspond mainly to the nearest contour points of the problematic points. Here also, we proceed iteratively until solving all the problematic points.

2.3. Adding information on the basis

In order to better constrain the basis, one can take advantage of additional information given for example by well logs or nearby outcrops, or even by considering a fault orientation that delimits a volcano. This information can be expressed as points or lines belonging to the basis. Since the method considers that the basis must pass through all the points of the contour and that the contour can be fragmented in several lines or sub-contours, we added these constraint points or lines as part of the contour. In the program, these additional points or lines are named “checkpoints”.

3. Validating the method with the Paricutin case

The Paricutin case is ideal to test our method as we know the previous topography. The volume computed as the elevation difference between the two topography inside the contour C_2 and multiplied by the internal area rounds 2.1 km^3 (see Table 1). It is taken as a reference when comparing the several strategies of our method. However, since most of the ash and tephra was blanketed far away from the Paricutin volcano, even reaching Mexico City (~ 350 km east of the volcano) during March-July, 1943 (Hernandez Velasco, 1945), the volume measured here is the volume of the nearby deposits and not the whole emitted volume. The 2.1 km^3 value is slightly higher than the value reported in (Larrea et al., 2017) since we have also considered tephra and volcanic reworked deposits and not only lava. We present in Figure3 different views and sections of the Paricutin in order to compare the effects of the different strategies. The blue line is according to the pre-eruption paleo-topography and the orange line is for the topography post-eruption.

When using the strategy S_1 with the lava contour C_1 (resp. C_2), we obtained about the third (resp. the half) of the reference volume, i.e. ~0,75 km^3 (resp. ~1,08 km^3). The strategy S_2 with the contour C_2 allows assessing a volume of about more than three quarters of the reference volume, i.e. ~1,71 km^3. Finally, the strategy S_3 with the contour C_2 is the only strategy which allows obtaining a volume comparable to the reference volume ~2,05 km^3. In fact, the error on the volume estimation, which is about 2%, is much lower than the error on the basement elevation that can reach 50 m (the thickness error can reach 30%) because the assessed basement elevation oscillates around the paleo-topography elevation.

This result shows the importance of assessing correctly the contour and to interpolate the surrounding slope. However here, the contour C_2 has been determined only according to a significant difference between the post and pre eruption and without considering the surrounding slope or field observations. We can see on the left part in Figure3F, that the slope is not assessed correctly mainly because the contour is mispositioned. Then, even if strategy S_3 allows correcting automatically some contour mispositioning, we can still improve the calculation by better determining the contour by using slope criteria (Favalli et al., 2009).

As shown in the several sections presented in Fig.3, the paleo topography is not horizontal, nor flat, as it is usually considered when calculating the volume with contour interpolation (strategy S_1 or following (Lahitte et al., 2012)). At the opposite, the eruptive vent of the volcano is located 420 meters above a topographic depression due to the nearby presence of an ancient volcano (vent visible in Figure1A, Figure3C and E) and a distal flank of the Tancitaro volcano. In general, many monogenetic volcanoes grow in faulting zones, where magma uses it as a pathway to rise to the surface. These faults are cortical weaknesses producing in some cases graben structures or can easily be eroded yielding to grooves and valleys. Hence, the importance to get more realistic paleomorphologies of pre-volcanic deposits reduces the error on volume calculation.

The volumes obtained from the two contours C_1 and C_2 reaches a factor 2. The correct determination of the contour is then fundamental and must correspond to the border of a depression that has been recovered. For recent eruptions however, this border might be recovered by tephra deposits since they can diffuse very far from the vent. They are produced by the deposition of pyroclasts from the eruptive plume or the volcanic cloud. The thickness of distal/middle-deposits is generally in good agreement with exponential or power law functions (Bonadonna & Houghton, 2005) and their volume can then also be assessed but is here beyond the scope of this study because of the poor vertical resolution. Nonetheless, the thin deposits are rapidly degraded and transported and will after some time allow the correct identification of the contour. We observed in the Paricutin case that a recent satellite observation of the deposits contour and of the vegetation allows situating a contour like C_2. We additionally measured the thickness of tephra deposits at several positions and concluded that a contour for thickness of about 2 m is also like C_2. In fact, to estimate the tephra-deposit dynamic and consecutively, the eruption magnitude, and the intensity of an explosive volcanic eruption, it is necessary to develop several isopach maps through time. For more former eruptions, when no clear evidence on the field allows determining the contour, or if a larger number of volcanoes must be processed automatically, another method consists in analyzing the slope variations of the volcanoes (Lahitte et al., 2012).

Table 1. Volume results according to the strategy and the contour

Volume method:	Using topographies pre and post eruption	S_1 with C_1	S_1 with C_2	S_2 with C_2	S_3 with C_2
Results: (km^3)	2.12	0.75	1.08	1.71	2.05

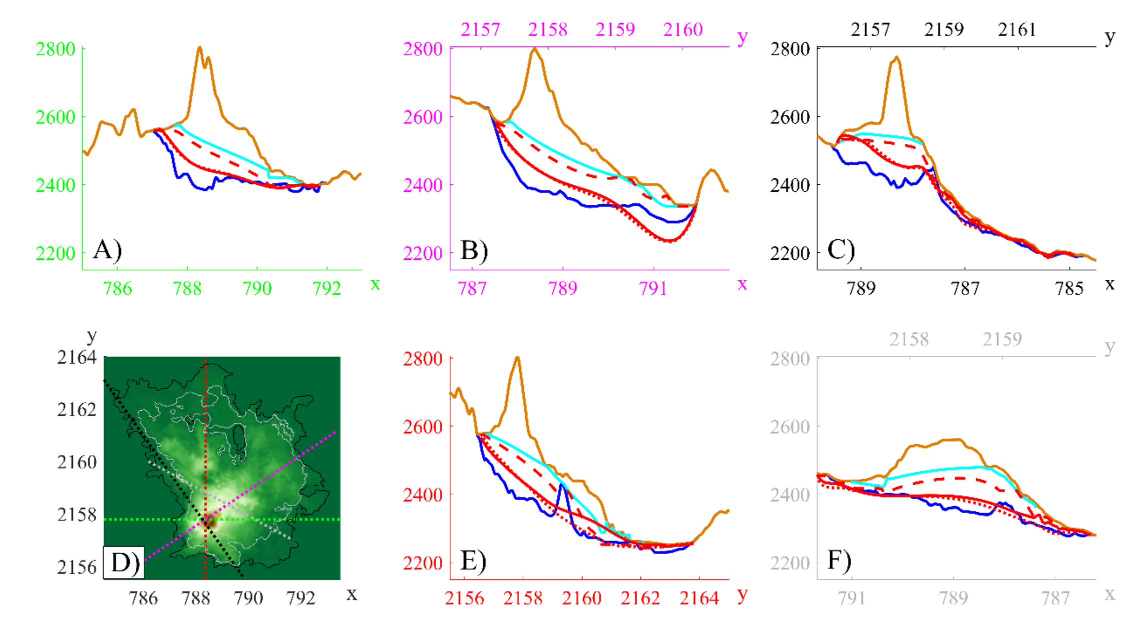

Figure3: D) top view of Paricutin volcano with the same color scale as in Figure1. Additionally, we superimposed dotted lines for the several sections presented in A), B), C), E) and F). The colors of the lines are the same as of the frame axes. On the sections, the thick blue line is according to the pre-eruption topography and the orange line is according to the post eruption topography. The sections of the basement obtained with the strategy S_1 with the lava contour C_1 (resp. C_2) are plotted as continuous lines of cyan color (resp. dashed lines of red color). The sections of the basement obtained with the strategy S_2 (resp. S_3) with the lava contour C_2 are plotted as continuous lines of red color (resp. dotted lines of red color). Axes x and y are expressed in km and elevation is in m.

4. Applying the method on superimposed volcanoes and lavas and comparison with another method

The method proposed here is also useful to determine finely the paleo topography to simulate the lava flow and potentially retrieve some lava parameters such as temperature, flow and viscosity at the eruption moment and better predict volcanic hazard (Mossoux et al., 2016). We can also better assess the volume of buried or partially recovered volcanoes as it is the case for the La Nieve volcanic complex shown in Figure4. The northern Nieve volcanic cluster encompasses an area of 450 km2 and it is formed by 20 domes, two cinder cones, and three lavas (Cardona Melchor, 2015). The contours were first identified during several field trips by surface observation, but 3D methods would certainly be more appropriate to identify the covered volcano contours. Common magnetic and seismic methods might provide this information but with an expansive cost. In contrast here, we assess several contours at no cost just from the DEM. For example, after determining the Isidro scoria cone (Is) basement, we assessed the paleo topography of the Yerbabuena Dome (Ye). In such a case, it was easy to recognize the new contour because several distinct parts were already identified. In another example, we also identified the whole Guadalupe dome (Gu) contour even partially recovered by La Nieve dome (Ni). When using this procedure, it is important to process the several volumes according to their age: the younger firsts and the older afterward. Other volcanoes (Bu, Ta) are also drawn with transparency in order to show that we extended below them the lavas of other volcanoes (Zi, Di, Pu, Gu, Um). A priori, we cannot extend the lava that has been several times recovered since the basements are slightly smoothed by the method. However, further verification of lava emplacement can be made using simulation of lava flow (Cisneros Máximo & Avellán López, 2018) in order to bring further constraints on their shape. In general, the extended parts contribute at maximum to 10% of the truncated volume.

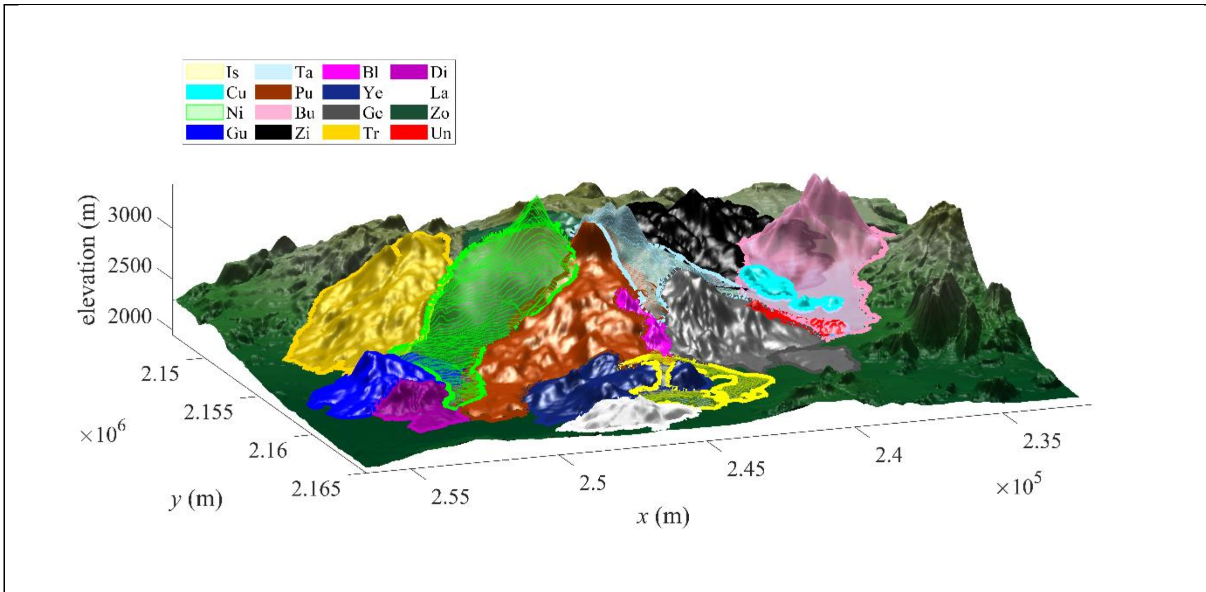

Figure 4: The Complejo volcánico La Nieve is made of several scoria or lava cones and domes (Is: Isidro scoria cone (21 ka), Cu: Cuanajo scoria cones (28 ka), Ni: La Nieve dome (88 ka), Gu: Guadalupe dome (140 ka), Pu: Los Puercos lava cone (370 ka), Ta: La Taza dome (370 ka), Bu: El Burro dome (700 ka), Zi: Zimbicho dome (1.3 Ma), Un: Unguarán dome (1.46Ma), Bl: Cerro Blanco dome (1.47 Ma), Ye: Yerbabuena dome (1.6 Ma), Ge: Genoveva dome (1.9 Ma), Tr: Trampa dome (2Ma), Di: Divisadero dome (2.6 Ma), La: Lagunillas lava cone (2.98 Ma), Zo: Zoromuata dome (3.8 Ma)). Is, Ni, Bu, and Ta are plotted with transparency to allow visualizing partially buried lavas underneath.

Another advantage of our method is its ability to determine the volume of lava flows. We present in Figure5 a lateral view of the Los Puercos lava cone: the lava stands on a steep slope and has a small thickness compared to its width and length. These characteristics and the presence of a depression in the middle or of a roll on the edge due to the viscosity of the lava make the volume computation generally a difficult task to determine with other methods.

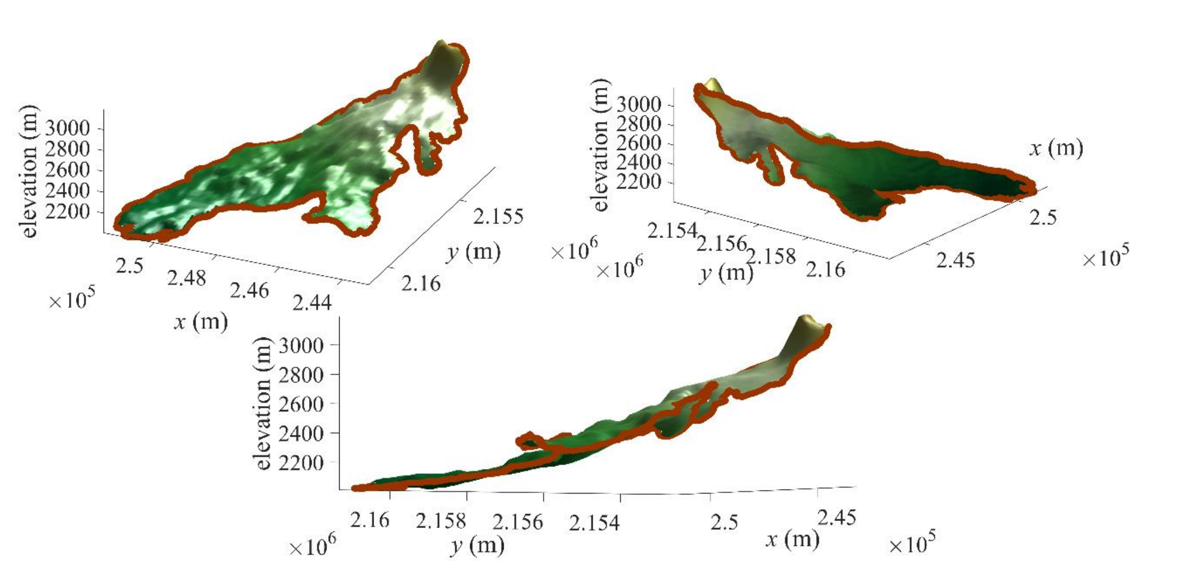

Figure5: Several views of the Los Puercos lava cone: the lava stands on a slope and has a small thickness compared to its width and length.

Finally, to demonstrate the potential of our method, we also calculated the volumes of the volcanoes of this complex using the “3D Analyst” module of (ArcGIS, 2014). In this software, the basement is first determined from linear interpolation between the points of the contour without resolution of the problematic points. Then, the DEMs of the basement and of the topography are converted to Triangular Irregular Network maps (TIN) which can be used with the tool “surface difference” to calculate the volumes. The results of this method are compared against the results obtained using our method in Table 2. In general, our method gives results 30% higher than those of ArcGIS method. This agrees with the conclusions of the previous section: the consideration of the surrounding slopes generally increases the volume with respect to the linear interpolation of the basement. It is also important to underline that our results have been processed in less than 3 minutes (without considering the contour identification) and that an experienced user lasted more than one day to process the volumes with ArcGIS.

Table 2: comparison of volcanoes volume computed with ArcGIS method and our method

Abbreviated volcano name	Volume computed using	
	ArcGIS (km^3)	our S_3 method (km^3)
Bl	0.05	0.06
Bu	1.97	3.59
Cu	0.08	0.05
Di	0.25	0.31
Ge	0.71	1.16
Gu	0.60	0.92
Is	0.18	0.22
La	0.33	0.35
Ni	1.89	3.31
Pu	0.78	1.67
Ta	0.65	0.87
Tr	0.89	1.3
Un	0.03	0.09
Ye	0.51	0.92
Zi	1.62	2.03
Zo	0.17	0.31
Total	10.75	17.13

5. Conclusions

The main contribution of our method is the consideration of a non-flat basis that results from the extrapolation of the slope outside the volcano. The motivation is to correct the apparition of negative volume due to a basis elevation that result above the actual volcano topography. This error generally arises when realizing a Delaunay triangulation of the contour, without considering the actual topography and the surrounding topography slopes. We validated this technique with the Paricutin case and assessed a volume of 2.05 km^3 close to the volume of 2.1 km^3 calculated from the difference between the pre-eruptive and post-eruptive topographies. We also presented the case of the Complejo volcánico La Nieve-El Burro where several volcanoes are imbricated and where we deduced several buried topographies. Finally, we compared the volcano volumes for this complex obtained by our method and by a module of ArcGIS and showed that our values are generally 30% larger since our method resolves negative volume problems.

Acknowledgments, Samples, and Data

Funding for this research was provided by Fronteras de la Ciencia project: 2016-01-2406 of CONACyT to J.L. Macías.

The software is named Volcalume and runs as Matlab executable under Linux, Windows or Mac. It has been developed by Mathieu Perton (mathieu.perton@gmail.com) in 2019. The size of the software is about 3.5 Mb but requires a free Matlab runtime of about 500 Mb and can be downloaded at: https://mathieuperton.github.io/Volcalume.html or https://zenodo.org/badge/latestdoi/351227199

The 1943 and 1952 Paricutin DEMs used in this article can be found in the program folder.

References

Albino, F., Smets, B., d'Oreye, N., & Kervyn, F. (2015). High-resolution TanDEM-X DEM: An accurate method to estimate lava flow volumes at Nyamulagira Volcano (D. R. Congo). *Journal of Geophysical Research: Solid Earth*, *120*(6), 4189–4207. https://doi.org/10.1002/2015JB011988

Amidror, I. (2002). Scattered data interpolation methods for electronic imaging systems: a survey. *Journal of Electronic Imaging*, *11*(2), 157–176. https://doi.org/10.1117/1.1455013

ArcGIS, (ESRI). (2014). *ArcGIS* (10.2). Environmental Systems Research Institute.

Bagnardi, M., González, P. J., & Hooper, A. (2016). High-resolution digital elevation model from tri-stereo Pleiades-1 satellite imagery for lava flow volume estimates at Fogo Volcano. *Geophysical Research Letters*, *43*(12), 6267–6275. https://doi.org/10.1002/2016GL069457

Bonadonna, C., & Houghton, B. F. (2005). Total grain-size distribution and volume of tephra-fall deposits. *Bulletin of Volcanology*, *67*(5), 441–456. https://doi.org/10.1007/s00445-004-0386-2

Cardona Melchor, S. (2015). *Evolución volcánica del Complejo Volcánico El Águila y los domos La Taza, La Nieve y El Burro, centro-norte de Michoacán*. Universidad Nacional Autonoma de Mexico.

Cisneros Máximo, G., & Avellán López, D. R. (2018). Parícutin el pasado y el presente: Simulación de flujos de lava con Q-LavHa. *Revista Científica de La Universidad Michoacana de San Nicolás de Hidalgo*, *74*, 59–80.

Cotton, C. A. (1944). *Volcanoes as Landscape Forms*. Whitcombe & Tombs limited.

Davidson, J., & De Silva, S. (2000). Composite Volcanoes. *Encyclopedia of Volcanoes,1*, 663–681.

Dibacto, S., Lahitte, P., Karátson, D., Hencz, M., Szakács, A., Biró, T., Kovács, I., & Veres, D. (2020). Growth and erosion rates of the East Carpathians volcanoes constrained by numerical models: Tectonic and climatic implications. *Geomorphology*, *368*, 107352. https://doi.org/10.1016/j.geomorph.2020.107352

Favalli, M., Karátson, D., Mazzarini, F., Pareschi, M. T., & Boschi, E. (2009). Morphometry of scoria cones located on a volcano flank: A case study from Mt. Etna (Italy), based on high-resolution LiDAR data. *Journal of Volcanology and Geothermal Research*, *186*(3–4), 320–330. https://doi.org/10.1016/j.jvolgeores.2009.07.011

Francis, P. (1993). *Volcanoes: A Planetary Perspective*. Oxford University Press. https://books.google.com.mx/books/about/Volcanoes.html?id=cF_wAAAAMAAJ&redir_esc=y

Germa, A., Lahitte, P., & Quidelleur, X. (2015). Construction and destruction of Mont Pelée volcano: Volumes and rates constrained from a geomorphological model of evolution. *Journal of Geophysical Research: Earth Surface*, *120*(7), 1206–1226. https://doi.org/10.1002/2014JF003355

Grosse, P., van Wyk de Vries, B., Euillades, P. A., Kervyn, M., & Petrinovic, I. A. (2012). Systematic morphometric characterization of volcanic edifices using digital elevation models. *Geomorphology*, *136*(1), 114–131. https://doi.org/10.1016/j.geomorph.2011.06.001

Hernandez Velasco, J. A. (1945). *Estudio de las cenizas del volcán caidas en la Ciudad de México: El Paricutin*.

Hildreth, W., Lanphere, M. A., & Fierstein, J. (2003). Geochronology and eruptive history of the Katmai volcanic cluster, Alaska Peninsula. *Earth and Planetary Science Letters*, *214*(1–2), 93–114. https://doi.org/10.1016/S0012-821X(03)00321-2

Hulme, G. (1974). The Interpretation of Lava Flow Morphology. *Geophysical Journal of the Royal Astronomical Society*. https://doi.org/10.1111/j.1365-246X.1974.tb05460.x

Kereszturi, G., Németh, K., Cronin, S. J., Agustín-Flores, J., Smith, I. E. M., & Lindsay, J. (2013). A model for calculating eruptive volumes for monogenetic volcanoes - Implication for the Quaternary Auckland Volcanic Field, New Zealand. *Journal of Volcanology and Geothermal Research*. https://doi.org/10.1016/j.jvolgeores.2013.09.003

Kubanek, J., Richardson, J. A., Charbonnier, S. J., & Connor, L. J. (2015). Lava flow mapping and volume calculations for the 2012–2013 Tolbachik, Kamchatka, fissure eruption using bistatic TanDEM-X InSAR. *Bulletin of Volcanology*, *77*(12), 1–13. https://doi.org/10.1007/s00445-015-0989-9

Lahitte, P., Samper, A., & Quidelleur, X. (2012). DEM-based reconstruction of southern Basse-Terre volcanoes (Guadeloupe archipelago, FWI): Contribution to the Lesser Antilles Arc construction rates and magma production. *Geomorphology*, *136*(1), 148–164. https://doi.org/10.1016/j.geomorph.2011.04.008

Larrea, P., Salinas, S., Widom, E., Siebe, C., & Abbitt, R. J. F. (2017). Compositional and volumetric development of a monogenetic lava flow field: The historical case of Paricutin

(Michoacán, Mexico). *Journal of Volcanology and Geothermal Research*, *348*, 36–48. https://doi.org/10.1016/j.jvolgeores.2017.10.016

Luhr, J. F., & Simkin, T. (1993). *Paricutin: The Volcano Born in a Mexican Cornfield.* Phoenix: Geoscience Press.

Martí, J. (2017). Assessing Volcanic Hazard : A Review. In *Oxford Handbooks Online* (Issue March 2018). https://doi.org/10.1093/oxfordhb/9780190699420.013.32

Matlab. (2020). *(R2020a)*. The MathWorks Inc.

Mossoux, S., Saey, M., Bartolini, S., Poppe, S., Canters, F., & Kervyn, M. (2016). Q-LAVHA: A flexible GIS plugin to simulate lava flows. *Computers and Geosciences*, *97*, 98–109. https://doi.org/10.1016/j.cageo.2016.09.003

Newhall, C. G., & Self, S. (1982). The volcanic explosivity index (VEI): an estimate of explosive magnitude for historical volcanism. *Journal of Geophysical Research*, *87*(C2), 1231–1238. https://doi.org/10.1029/jc087ic02p01231

Rodriguez-Gonzalez, A., Fernandez-Turiel, J. L., Perez-Torrado, F. J., Gimeno, D., & Aulinas, M. (2010). Geomorphological reconstruction and morphometric modelling applied to past volcanism. *International Journal of Earth Sciences*. https://doi.org/10.1007/s00531-008-0413-1

Rodriguez-Gonzalez, A., Fernandez-Turiel, J. L., Perez-Torrado, F. J., Paris, R., Gimeno, D., Carracedo, J. C., & Aulinas, M. (2012). Factors controlling the morphology of monogenetic basaltic volcanoes: The Holocene volcanism of Gran Canaria (Canary Islands, Spain). *Geomorphology*. https://doi.org/10.1016/j.geomorph.2011.08.023

Romano, R., & Sturiale, C. (1982). The historical eruptions of Mt. Etna (volcanological data). *Memorie Della Societa Geologica Italiana*, *23*.

Segerstrom, K. (1950). Erosion studies at Parícutin, State of Michoacán, Mexico. *U.S. Geological Survey Bulletin*, *965A*, 1–164. https://agris.fao.org/agris-search/search.do?recordID=US201300538398

Stevens, N. F., Wadge, G., & Murray, J. B. (1999a). Lava flow volume and morphology from digitised contour maps: A case study at Mount Etna, Sicily. *Geomorphology*, *28*(3–4), 251–261. https://doi.org/10.1016/S0169-555X(98)00115-9

Stevens, N. F., Wadge, G., & Murray, J. B. (1999b). Lava flow volume and morphology from digitised contour maps: A case study at Mount Etna, Sicily. *Geomorphology*. https://doi.org/10.1016/S0169-555X(98)00115-9

Székely, B., & Karátson, D. (2004). DEM-based morphometry as a tool for reconstructing primary volcanic landforms: Examples from the Börzsöny Mountains, Hungary. *Geomorphology*, *63*(1–2), 25–37. https://doi.org/10.1016/j.geomorph.2004.03.008

Thouret, J.C. (1999). Volcanic Geomorphology-An Overview. *Earth-Science Reviews*, *47*, 95–131. https://es.scribd.com/document/46352785/Thouret-1999-Volcanic-Geomorphology-An-Overview

Thouret, Jean Claude, Oehler, J. F., Gupta, A., Solikhin, A., & Procter, J. N. (2014). Erosion and aggradation on persistently active volcanoes—a case study from Semeru Volcano, Indonesia. *Bulletin of Volcanology*, *76*(10). https://doi.org/10.1007/s00445-014-0857-z

Wadge, G., Walker, G. P. L., & Guest, J. E. (1975). The output of the Etna volcano. *Nature*, *255*(5507), 385–387. https://doi.org/10.1038/255385a0

Wilson, L., & Head, J. W. (1983). A comparison of volcanic eruption processes on Earth, Moon, Mars, Io and Venus. In *Nature*. https://doi.org/10.1038/302663a0

Wood, C. A. (1980). Morphometric evolution of cinder cones. *Journal of Volcanology and Geothermal Research*. https://doi.org/10.1016/0377-0273(80)90040-2